Indonesian Journal of Electrical Engineering and Computer Science
Vol. 3, No. 1, July 2016, pp. 80 ~ 90
DOI: 10.11591/ijeecs.v3.i1.pp80-90

Investigations of Electrostatic and Ionized Fields Analysis for Dual-Electrode System

Mohamed A. Abouelatta*, Abdelhadi R. Salama, A. M. Omar, S. A. Ward
Shoubra Faculty of Engineering, Benha University, 108 Shoubra St., Cairo, Egypt
*Corresponding author, e-mail: moh_an1@yahoo.com

Abstract

The paper presents the computation and measurement of electric field, in both electrostatic as well as ionized case, for dual electrode system intended for electrostatic applications. The dual electrode system consists of an ionizing and non-ionizing electrode have the same voltage and facing a grounded collecting plate. The charge simulation method (CSM) coupled with genetic algorithms (GAs) and method of characteristic (MOC) is applied to compute the electrostatic field and the ionized field respectively. The influence of dual system parameters such as ionized wire diameter and inter electrode distances on the profile of the electrostatic field on the collecting plate and on the surface of the ionizing wire has been studied. The measurements of the ionized electric field, current-voltage characteristics and ion current density profiles are implemented using the technique of the linear biased probe. An experimental setup is constructed to model the present electrode arrangement. The measurements are carried out for ionized wire of diameter 0.25 and 0.5mm. The computed results are found to be in good agreement with experiments.

Keywords*: corona discharge, dual electrode system, linear biased probe, electric field.*

1. Introduction

The corona discharge employed in electrostatic approaches is useful in many applications such as dust precipitation, powder spraying, or granular mixtures separation by utilizing the electric forces exerted on such charged particles [1-6]. The region in which the electric forces act is widening by using a non-ionizing electrode with an ionizing electrode, dual electrode, resulting in the so called the corona-electrostatic field [7]. Several types and shapes of electrodes have been carried out experimentally to study these corona electrostatic fields, but they were very complex and expensive due to the presence of many parameters involving such fields [3, 4]. Besides, there was another trend to simulate the phenomena of corona charging and particle motion in electric fields in the presence of space charge by numerical model [4-7].

Accurate calculations and measurements of such fields are one of the major problems facing the designers of such electrostatic applications. Several analytical techniques have been applied by using different numerical models for such situations based on techniques such as the charge simulation method (CSM), finite differences (FDM), finite element (FEM), and the integrated method of finite element and the method of characteristics (MOC) [7-12]. Although various computational tools are developed for electric field calculations, none of them is mutable enough to be employed for the analysis of more complicated electric field configurations.

Many experiments had been carried out to measure the electric field in the presence of the ionic space charge field, but they are very complicated to get accurate measurements. The biased current probe is one of the procedures to measure the ionized electric field introduced by Tassiker [13] and then developed by selim and waters [14]. It consists of a linear biased probe and a rectangular collecting plate surrounded by a bias plates at voltage V_b. The operation of the linear biased probe is as follows [15]:

1. During corona discharge, the collector probe collects the current resulting from this discharge (I_o) when no bias voltage is applied to the bias plates.
2. This current (I_o) is reduced to I when the bias voltage V_b is applied to bias plates such that it produces a biased field that opposes the original unknown field E, so:

Received February 2, 2016; Revised May 25, 2016; Accepted June 10, 2016

$$\frac{I}{I_o} = f_{-}(V_b, E) < 1 \quad (1)$$

3. This current (I_o) is increased to I when the bias voltage V_b is applied to bias plates such that it produces a biased field that will aid the original unknown field E, so:

$$\frac{I}{I_o} = f_{+}(V_b, E) > 1 \quad (2)$$

The unknown electric field, E, can be known by measuring (I_o) and (I) in aiding and opposing bias operations if f_- (V_b, E) and f_+ (V_b, E) are known.

In this paper, firstly the present work is to validate a numerical model capable of computing the electrostatic field distributions in ''dual electrode'' configurations using CSM coupled with GA. Secondly, a numerical technique is presented based on the combined method of CSM and MOC to evaluate ionized fields in such geometries. An experimental setup is constructed to model the present electrode arrangement. The linear biased probe is implemented to measure the ionized electric field, current-voltage characteristics and current density distribution in dual electrode systems. The total ionic current produced by the corona discharge is calculated for different values of the potential applied to the ionizing electrode. The results of the numerical simulation and the experimental measurements demonstrate the effectiveness and accuracy of the proposed approach.

2. Corona Model of Dual Electrode System

2.1. Physical Model

The corona discharge, for any form or sort of ionizing electrode, is normally marked by the presence of two regions: the ionized thin layer and the drift zone. To formulate the corona discharge in a simple way, the study related to corona discharge is reduced to the estimation of the space charge density imported from the unipolar ions passing along the field lines and comes only from the ionized thin film layer. This method is implemented to represent the corona model influenced by the ionic space charge [16].

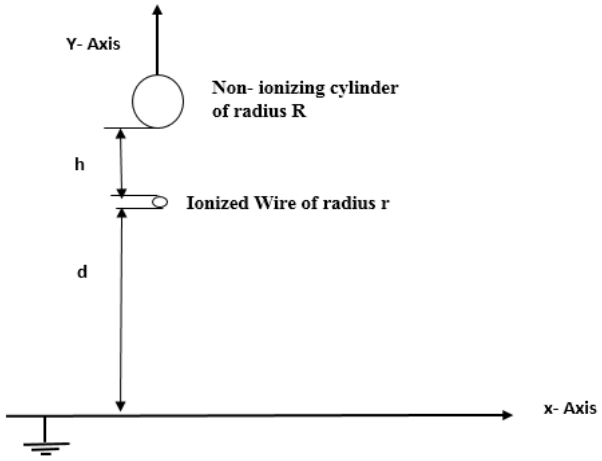

Figure 1. Dual Electrode Configuration.

The proposed electrode configuration is shown schematically in Figure 1. The physical model of the corona discharge assumes that:

a. The wire and the cylinder are all at the same applied negative potential V.
b. The ground plate electrode is at zero potential.
c. The corona discharge is supposed to take place only at the ionizing wire surface and the large cylindrical electrode is assumed to be in non-ionizing state.

d. The unipolar ions migrate from the surface of the ionizing wire towards the grounded plate in the combined field established by the two electrodes with constant mobility k.

The medium in which the electrodes are situated is air such that D = ε0E, where D and E are the electric displacement and the field strength, respectively, and ε0 is the vacuum permittivity.

2.2. Governing Equations and Boundary Conditions

The calculation is transferred to two-dimensional domain by ignoring the edge effect of the electrodes and assuming constant and uniform corona discharge. The governing equations defining the electric field E in the presence of the negative ions are as follows [16]:

Poisson equation:

$$\Delta V = - \rho / \varepsilon_0 \quad (3)$$

Where, ρ is the ionic space charge density and V is the electric potential and, Electric field:

$$E = - \nabla V \quad (4)$$

The Current continuity equation:

$$\nabla . j = 0 \quad (5)$$

Where, $j = \rho k E$ is the corona current density and k is the ion mobility in m^2/Vs. The electrostatic field is computed by Laplace's equation:

$$\Delta V=0 \quad (6)$$

For the continuity Equation (5), the boundary condition consists in imposing a charge density value at all emitting points on the wire surface $\rho_0(\Omega)$. The method that permits to establish the value of ρ_0 (Ω) at each emitting point is based on the Kaptzov's assumption and Peek's relation [17]:

$$E_{on} = 31 \delta (1+ 0.308/r^{1/2}) \quad (7)$$

Where, E_{on} is the corona onset field in kV/cm, δ is the air density and r is the radius of the wire in cm.

3. Electrostatic Field Computation (CSM-GA)

To calculate the ionized fields of the dual electrode arrangement, Figure 1, the electrostatic field must be computed first. Charge simulation method (CSM) is implemented to calculate the symmetrical 2-D electrostatic electric field based upon Equation (4) [8]. A set of Ns simulating line charges is positioned at the inner surfaces of the energized electrodes. An equal number of contour points is selected along these surfaces. Equation (8) is constructed and solved to determine the magnitude of the simulation charges Q:

$$[P] [Q] = [V] \quad (8)$$

$$[FX][Q]= [E_X] \quad (9)$$

$$[F_Y] [Q]= [E_Y] \quad (10)$$

Where P is the potential coefficient matrix determined by the location of the charges and the contour points, Q is the unknown charges vector; V is the known potentials vector at the contour points. F_X and F_Y are the electric field intensity coefficients between the simulation charges and the electric field intensity components at the point where this field is calculated. E_X and E_Y are the components of the electric field intensity at the same point.

Eight and twenty four line charges are placed inside the ionizing wire and inside the cylindrical electrode on hypothetical cylindrical surfaces of diameters $2r_1*f_1$ and $2R*f_2$ respectively. A range between 0 and 1 is taken for the optimization parameters values f_1, f_2. The method of image is applied to simulate the ground plate. An algorithm which couples genetic algorithms and the charge simulation method is developed, in the MATLAB environment, in order to determine the fitness function (FF) given by;

$$FF = \sum_{j=1}^{N_h} \left[V - v_j \right]^2 \quad (11)$$

Where, V is the electrode voltage (1 p.u) and v_j is the potential obtained by the CSM at the check point j.

The calculations are terminated when a pre-specified number of generations are reached. The sequence of the proposed GA-CSM flowchart is illustrated in Figure 2. Details of GA operations and implementations are given in [18-20].

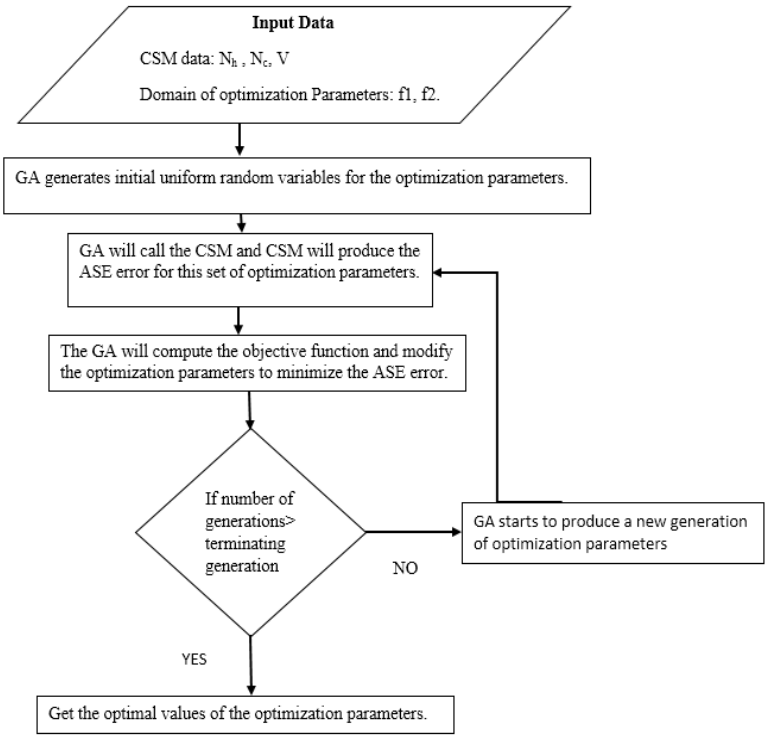

Figure 2. Flowchart of the GA-CSM Algorithm

4. Ionized Electric Field Calculation (MOC/CSM)

Several techniques had been earlier suggested to compute the corona discharges governing equations for different geometries [7-12]. The combined technique of the Method of Characteristics and the Charge Simulation Method (MOC/CSM) is implemented to solve the corona problem of the dual electrode configuration given by Equation (3-5). CSM is used to solve Equation (3) and (4), while MOC is implemented to solve Equation (5). Both problems are solved iteratively until the solution of the system of equations is reached [11]. The techniques' goal is to perform a self-consistent solution of the electric field and the space charge distribution. A two-nested loop algorithm is proposed. Inside the inner loop, the spatial distributions of the electric field and space charge density are renewed at the end of the loop [10]. The computational operation persists with the charge distribution, at any point on the wire surface, being modified in an outer loop until the computed field on the ionized wire surface is

equal to the onset value. The boundary conditions of the problem are summarized as follows [4]:

a. The points along the surface of the non-ionized cylinder and the ionized wire have the same potential equal to the applied voltage, V.
b. The points along the collecting plate surface are at zero potential.
c. A non-uniform charge distribution on the surface of the ionizing wire is assumed.
d. The electric field is equal to the corona onset field at all points along the surface of the ionizing wire.

A flowchart of the proposed algorithm is shown in Figure 3 [10].

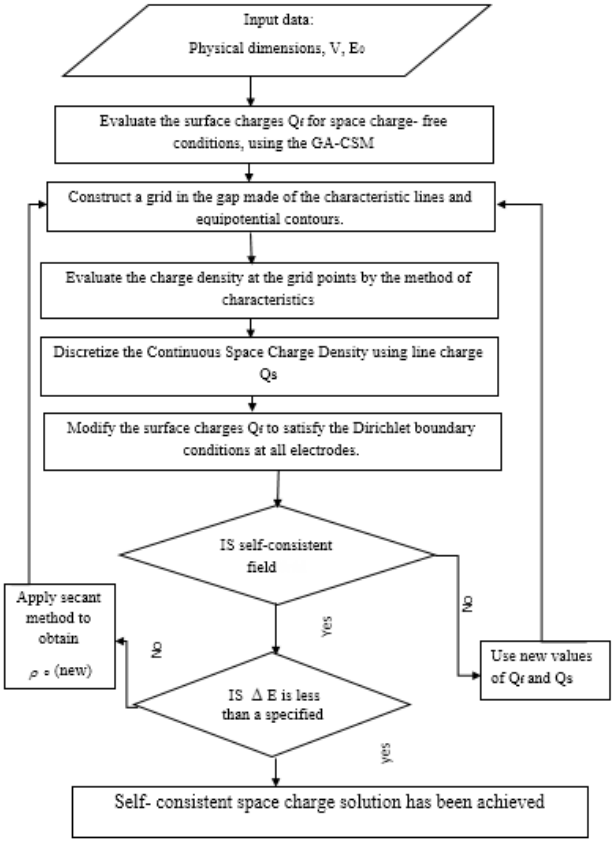

Figure 3. Flowchart for Computations of the Ionized Fields

5. Design of the Linear Probe System

The developed linear probe system is applied for ionized electric field strength and current density measurements. The ground plate of the experimental setup is designed as double sided PCB. A plan view of the top and bottom layer is shown in Figure 4a, Figure 4b. The top layer consists of a probe collector (A), two bias plates (B, B) and four guard planes (C, C, C', C'). The bottom layer consists of three plates (1, 2, 3). Plates A, B, C, C', 1, 2 and 3 are made of copper. To avoid any leakage currents could emerge from the bias plates or the high voltage ionized wire and might affect the measurements' accuracy, the probe needs neat design. The leakage current evolved from the bias plates is prevented by using copper plate (2) while the leakage current between the high voltage wire and the probe is taken to earth by the guard planes (C').

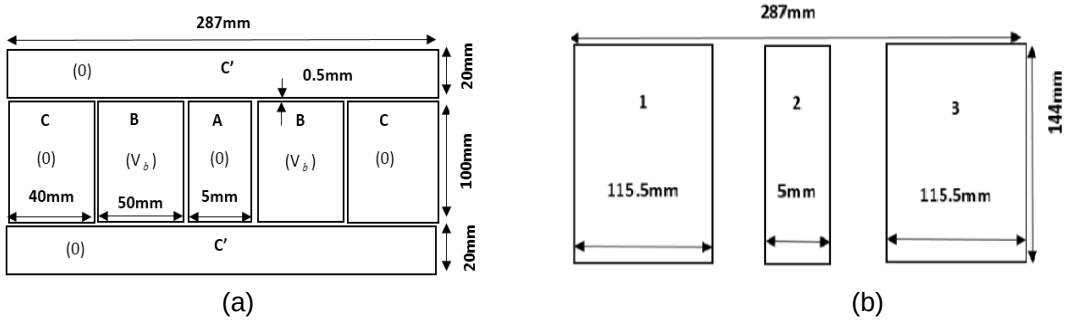

Figure 4. Variation of Electrostatic Field (a) Top Layer of the Ground Plate (b) Bottom Layer of the Ground Plate

6. Experimental Procedure

The experimental set-up for the measurement of current–voltage characteristics of the corona wire, ionized electric field distribution and for the study of the corona current density distribution at the surface of the grounded electrode is exhibited in Figure 5. A tungsten wire is hanged parallel to and above the ground plate described in the above section. The wire is located at a distance, d, equal to 25 mm from the surface of the grounded plate and is fixed by a non-ionizing cylinder of circular cross section (radius R = 12.5 mm). The spacing between the wire and the non -ionized cylinder, h, is 20 mm. The electrodes were injected from a negative DC high-voltage supply (Hipotronics model 800pl- 10mA, 0-80kV) and the bias plates (B) are connected to a DC low voltage source (Model ED-345B).

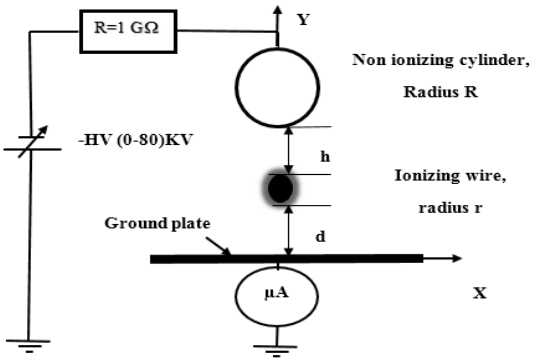

Figure 5. Variation Experimental Setup

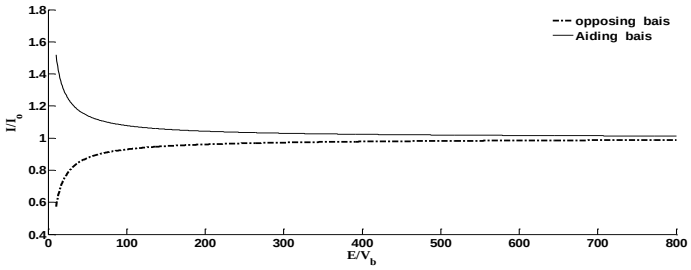

Figure 6. Variation Calibration Curves for Ionized Electric Field Measurements

Calibration curves $I/I_o = f(E / V_b)$ are built for the designed probe depending on the analytical model of the linear probe mentioned in [15]. Figure 6 identifies the global curves constructing the normalized field $En = E/V_b$. The unknown field (E) is therefore obtained as $E = V_b.E_n$, where the value of E_n is determined from the curves and V_b is taken equal to ± 50V. The

procedure is auto-confirming as changing the bias voltage V_b, should give a constant value of field intensity E.

7. Results and Discussion

The effect of changing the ionized wire diameter upon the lateral electrostatic field strength on the ground plate and around the ionized wire is presented in Figure 7. As the wire diameter increases higher electric field strength is realized, Figure 7a. The fig. also outlines a symmetrical field distribution around the vertical wire axis. It is obvious that the maximum value of the ground field strength, E_{gm}, is exactly under the wire (x = 0). The influence of the wire diameter variation upon the electric field strength is almost sprinkling far away from the vertical wire axis.

The electrostatic field upon the wire surface decreases with increasing the ionized wire diameter, Figure 7b. The minimum value of the electrostatic field, E_{wi}, is obviously located at the top of the ionized wire. An increased non-uniformly field is identified around the wire surface and reached its maximum value, E_{wm} in the region facing the ground plate (θ=2700). The value of E_{wm} for 1mm wire diameter increases by 21.793%, 62.875% and 175.648% when the wire diameter decreases to 0.75mm, 0.5mm and 0.25mm respectively. The maximum variation between E_{wi} and E_{wm} increases as the wire diameter increases. The variation is 9.15% for 0.25mm wire diameter and increases by 15.35%, 20.3806% and 24.64% when wire diameter increases to 0.5mm, 0.75mm and 1mm respectively. These results identify a non-uniform field distribution around the wire.

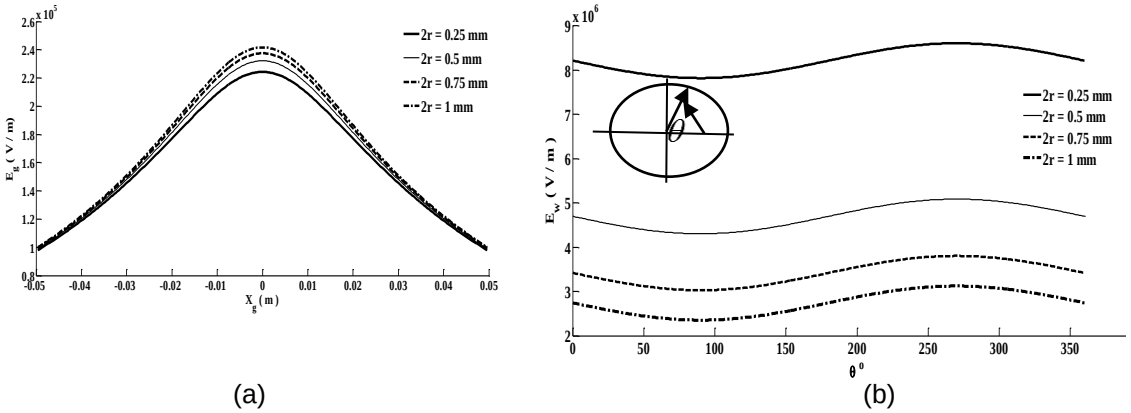

Figure 7. Variation of Electrostatic Field for Different Wire Diameters (V= 10kV, d= 25mm, h = 20mm); (a) On the Ground Plate, (b) Around the Ionized Wire

Figure 8 shows the variation of the electrostatic field upon the ground plate and around the ionized wire for reasonable distances d between 23-31mm. The field strength upon the ground plate strongly decreases as the ionized wire gets far away from the ground plate, Figure 8a. It was noticed that E_{gm} for d=29mm is increased by 7.2278%, 15.57% and 25.3024% when d decreases to 27, 25 and 23 mm respectively.

The electrostatic field upon the ionized wire surface increases with decreasing d, Figure 8b. The value of E_{wm} for d=29mm increases by 3.1718%, 6.71% and 10.68% when d decreases to 27, 25 and 23 mm respectively. The maximum difference between E_{wi} and E_{wm} decreases as d increases. This difference is 15.479% for d=23mm and decreases to 15.353%, 15.244% and 15.147% when d increases to 25mm, 27mm, 29mm respectively.

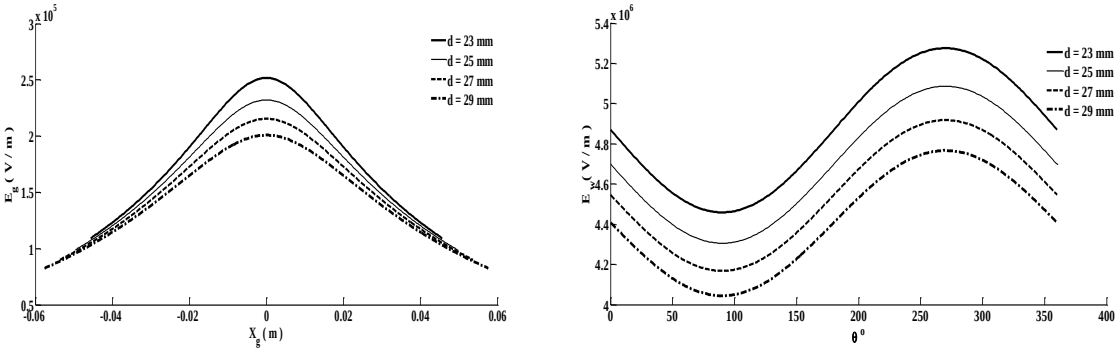

(a) (b)

Figure 8. Variation of Electrostatic Field for Different Ionized Wire Distances, d, (V= 10kV, r= 0.25mm, h = 20mm); (a) On the Ground Plate (b) Around the Ionized Wire

The influence of the inter electrode distance, h, on the electrostatic field upon the ground plate and around the ionized wire is illustrated in Figure 9. The field strength upon the ground plate is highly decreased as the non-ionized cylinder gets far away from the ionized wire, Figure 9a. The value of E_{gm} for h equals 40mm is increased by 5.3276%, 12.9616% and 25.0328% when h decreases to 30, 20 and 10 mm respectively.

The electric field upon the wire surface increases with increasing h, Figure 8b. The value of E_{wm} for h=10mm increases by 22.2946 %, 35.1477% and 43.62512% when h increases to 20, 30and 40 mm respectively. The maximum variation between E_{wi} and E_{wm} decreases as height, h, increases. This difference is 26.3434% for h=10mm and decreases to 15.3539%, 11.0720% and 8.8140% when h increases to 20mm, 30mm and 40mm respectively.

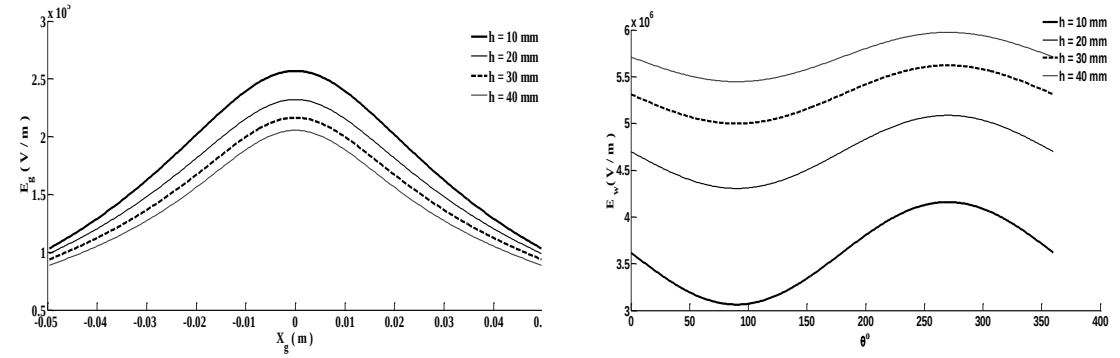

(a) (b)

Figure 9. Variation of Electrostatic Field for Different Inter Electrode Distances, h, (V= 10kV, r= 0.25mm, d =25mm); (a) On the Ground Plate (b) Around the Ionized Wire

The computed and measured current- voltage characteristics of the proposed dual electrode geometry for two different wire diameters are shown in Figure 10. The corona onset voltages for 0.25mm and 0.5mm wire diameters are 13kV and 16kV respectively. For a given value of applied voltage, the corona current increases when the wire diameter decreases. The Experimental measurements are in good agreement with the numerical results. The different between the numerical results and the measured ones does not exceed 10%. For small voltages, the experimental measurements underestimated the numerical computations.

Figure 11 displays the variation of computed and measured values of ionized electric field strength at the surface of the grounded plate. As the wire diameter decreases, higher electric field values are obtained and wider distributions are produced. It is confirmed that the ion space charge presence increases the electric field strength at the ground plate comparing

with no free space charge field. Experimental measurements agree well with the results obtained using the developed numerical algorithm. The computed electric field values differ by less than 3% from the measured one.

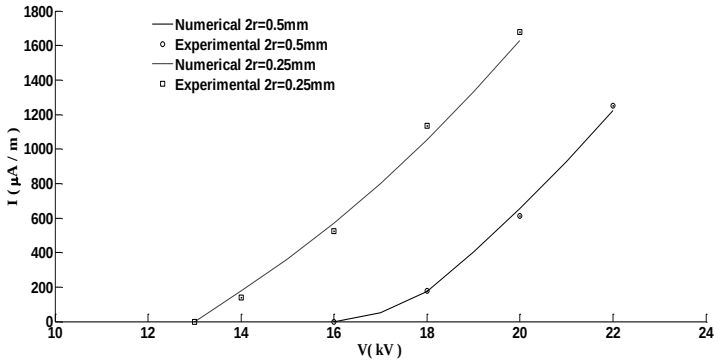

Figure 10. Corona V-I Characteristics of the Electrode Configuration (d = 25mm, h=20mm)

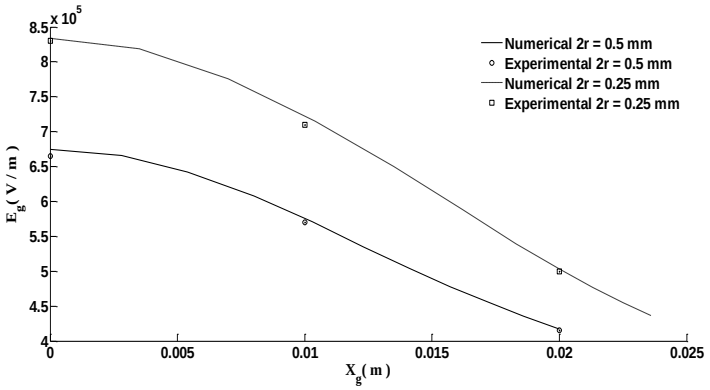

Figure 11. Variation of Ionized Electric Field on the Ground Plate (V= 20 kV, d = 25mm, h=20mm)

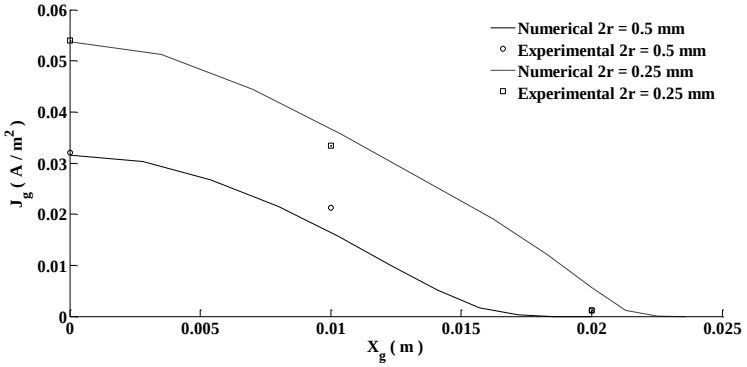

Figure 12. Variation Current Density Distributions at the Surface of the Grounded Plate (V = 20 kV, d = 25 mm, h=20mm)

The corresponding computed and measured current density distributions are indicated in Figure 12. For an applied voltage of 20 kV, the maximum current density, Jgm, grows by

about 70.25% when wire diameter decreases from 0.5 mm to 0.25 mm and the spatial extension of theses quantities becomes larger. Experimental measurements were in good agreement with the computed results obtained using the developed numerical algorithm. The different between the numerical results and the measured ones does not overstep 10%.

5. Conclusion

a. Experimental and numerical investigations of electrostatic and ionized field for dual electrode system intended for electrostatic applications have been presented.
b. The charge simulation method (CSM) coupled with genetic algorithms (GAs) and method of characteristic (MOC) is employed to compute the electrostatic field and the ionized field respectively.
c. The influence of various dual system parameters on the profile of the electrostatic field on the ground plate and on the surface of the ionizing wire has been investigated.
d. It was observed that reducing the ionized wire diameter increases the maximum electric field upon the ionized wire surface E_{wm} and decreases the maximum electric field strength on the ground plate E_{gm}. Also the non-uniformity around the wire was increased by increasing the wire diameter.
e. It was found that E_{gm} is increased by decreasing inter-electrode distance h, while E_{wm} is decreased by decreasing h.
f. It was noticed that E_{gm} and E_{wm} are decreased by increasing the position of ionized wire, d. It is clear that the non-uniformity around the ionized wire decreases as d increases.
g. The measurements of the ionized electric field and ion current density profiles are developed using the technique of the linear biased probe. An experimental setup was prepared to model the dual electrode arrangement.
h. The maximum current density and the maximum ionized electric field at the ground electrode surface were grown by decreasing the ionized wire diameter.
i. The experimental results were conformed to the computed results using the developed numerical algorithm.

References

[1] Dumitran L, Samuila A, Notingher P, Dascalescu L. *Electrostatic separation of polymeric granular mixtures from medium and low voltage cables.* 9th International Symposium on Advanced Topics In Electrical Engineering. Bucharest, Romania. 2015.
[2] Moore A. Electrostatics and its Applications. New York: Wiley. 1973.
[3] Younes A, Younes M, Sayah H, Samuila A, Dascalescu L. Experimental and numerical modeling of a new tribo- electrostatic separation process for granular plastics mixtures. *International Journal of Particulate Science and Technology.* 2015; 33(2): 189-196.
[4] Abouelsaad M, Abouelatta M, Salama A. Experimental and numerical investigations of the corona characteristics of a new Tri-electrode system for electrostatic separation processes. *European Physical Journal Applied Physics*. 2014; 67(3): 3080:1-11.
[5] Kachi M, Dascalescu L. Corona discharges in asymmetric electrode configurations. *Journal of Electrostatics*. 2014; 72(1): 6-12.
[6] Dumitran L, Badicu L, Plopeanu M Dascalescu L. Efficiency of dual wire cylinder electrodes used in electrostatic separators. *Revue Roumain des Sciences Techniques*. 2010; 55(2): 171-180.
[7] Dumitran L, Pierre A, Notingher P, Dascalescu L. 2-D corona field computation in configurations with ionizing and non-ionising electrodes. *Journal of Electrostatics*. 2006; 64(3): 176-186.
[8] Abouelsaad M, Abouelatta M, Salama A. Genetic algorithm-optimised charge simulation method for electric field modelling of plate-type electrostatic separators. *Science, Measurement & Technology IET*. 2013; 7(1): 1-7.
[9] Yanallah K, Pontiga F, Castellanos A. Numerical simulation of an oxygen-fed wire-to-cylinder negative corona discharge in the glow regime. *Journal of Physics D: Applied Physics. 2*011; 44(5): 1-21.
[10] Abdel-Salam M, Hashem A, Turky A, Abdel Aziz A. Corona performance of conductor-to-plane gaps as influenced by underneath grounded and negatively stressed metallic grids. *Journal of Physics D: Applied Physics. 2*007; 40(6): 1684-1693.
[11] Elmoursi A. Simulation of space charge in unbounded geometries. *IEEE Transactions on Industry Applications*. 2007; 26(2): 384-392.

[12] Davis J, Hoburg J. Wire-duct precipitator field and charge computation using finite element and characteristics methods. *Journal of Electrostatics*. 1983; 14(2): 187-199.
[13] Tassicker J. *Boundary probe for measurement of current density and electric field strength with special reference to ionised gases.* Proceedings of IEE. 1974; 121(3): 212-220.
[14] Selim O, Waters T. Static probe for electrostatic field measurement in the presence of space charge. *IEEE Transactions on Industry Applications*. 1980; 16(3): 458-463.
[15] Bouziane A, Hartmann G, Hidaka K, Taplamaci C, Waters T. Linear geometry electric-field probe for DC corona measurement. *European Physical Journal Applied Physics*. 1999; 6(2): 195-203.
[16] Sigmond S. The unipolar corona space charge flow problem. *Journal of Electrostatics*. 1986; 18(3): 249-272.
[17] Peek F. Ionisation Phenomena in High Voltage Engineering. New York: McGraw-Hill. 1929.
[18] Goldberg D. Genetic algorithms in search, optimization, and machine learning. Addison-Wesley. 1989.
[19] Sivanandam S, Deepa S. Introduction to genetic algorithms. Berlin: Springer. 2008.
[20] Haupt R, Werner D. Genetic algorithms in electromagnetic. New Jersey: John Wiley &Sons. 2007.